



## WEDNESDAY SLIDE CONFERENCE 2022-2023

Conference #21

29 March 2023

### CASE I:

#### **Signalment:**

12-year-old, male neutered, Havanese dog  
(*Canis familiaris*)

#### **History:**

A 12-year-old, male neutered Havanese dog has been managed through the Neurology Service over the course of 2 years for a right forebrain mass and cluster seizures. The dog was treated with radiation therapy 2 years ago and continued to have seizures. More recently, the dog started showing progressive neurologic signs consistent with regrowth of the mass (more frequent seizures, circling to the right, dull mentation, decreased menace OS). The dog presented to the Neurology service for cluster seizures and was hospitalized for seizure management. The seizures could only be controlled with a valium CRI. His owners elected euthanasia given the persistent breakthrough seizure activity and progressive neurologic dysfunction.

#### **Gross Pathology:**

The right frontal lobe has a focal, firm, tan, irregular mass that is adhered to the regional dura and measures 2.3 x 3 x 3.3 cm. The regional cerebral gyri are expanded (edema). Impression smears are obtained.

The fixed brain is sectioned. In the right frontal lobe, there is an irregular, firm, tan mass with a midline shift and regional parenchymal expansion.

#### **Laboratory Results:**

Impression smear cytology of brain mass: Smears are highly cellular and contain large numbers of round, oval and polygonal cells with abundant cytoplasm and well-defined cell borders. Cells contain large amounts of finely granulated, eosinophilic to amphophilic or basophilic cytoplasm. Nuclei are frequently eccentrically placed, round to oval and monomorphic with single or indistinct nucleoli. There is marked anisocytosis and mild anisokaryosis.

#### **Microscopic Description:**

One section of rostral cerebrum is examined. Extending from and expanding the leptomeninges, infiltrating into the regional cerebral cortex, there is a plaque-like, irregular, unencapsulated, mildly infiltrative neoplasm measuring approximately 1.8 x 1.0 cm. The neoplasm is comprised of large round, oval and polygonal cells forming sheets and supported by a scant, fibrovascular stroma. Neoplastic cells have well defined cell borders and contain abundant cytoplasm with densely packed eosinophilic granules. Nuclei are frequently eccentric, round, oval and sometimes angular, exhibiting mild pleomorphism (up to 2-fold) with finely stippled chromatin and an indistinct or single central nucleolus. There are zero mitoses in ten 40x (2.37 mm<sup>2</sup>) high power fields. The leptomeninges within and around the tumor undergoes fibrosis, with multifocal regions of chondroid metaplasia. The regional infiltrated cortex exhibits parenchymal rarefaction, vacuolation, increased

numbers of small caliber vessels lined by hypertrophied endothelial cells, increased numbers of glial cells comprised of microglial (including Gitter cells) and astrocytes. Multifocally, dilated, eosinophilic axons are observed (spheroids). Occasional foci of karyorrhectic debris, amorphous eosinophilic material and hemorrhage are present (necrosis). Rare perivascular aggregates of inflammatory cells are observed throughout the parenchyma and leptomeninges, comprised of lymphocytes, plasma cells and fewer macrophages containing golden brown, granular pigment (hemosiderin). Small vessels are infrequently mineralized.

**Contributor's Morphologic Diagnoses:**

Brain (rostral cerebrum): Granular cell tumor with regional infiltration, edema, gliosis, and leptomeningeal fibrosis with chondroid metaplasia

Special stains: Cytoplasmic granules are PAS positive and diastase resistant

**Contributor's Comment:**

Granular cell tumors (GCTs) are most common in the meninges of the cerebrum in dogs.<sup>2</sup> In dogs, these tumors are typically supratentorial and extra-axial, plaque-like and infiltrative, however, can also cause diffuse

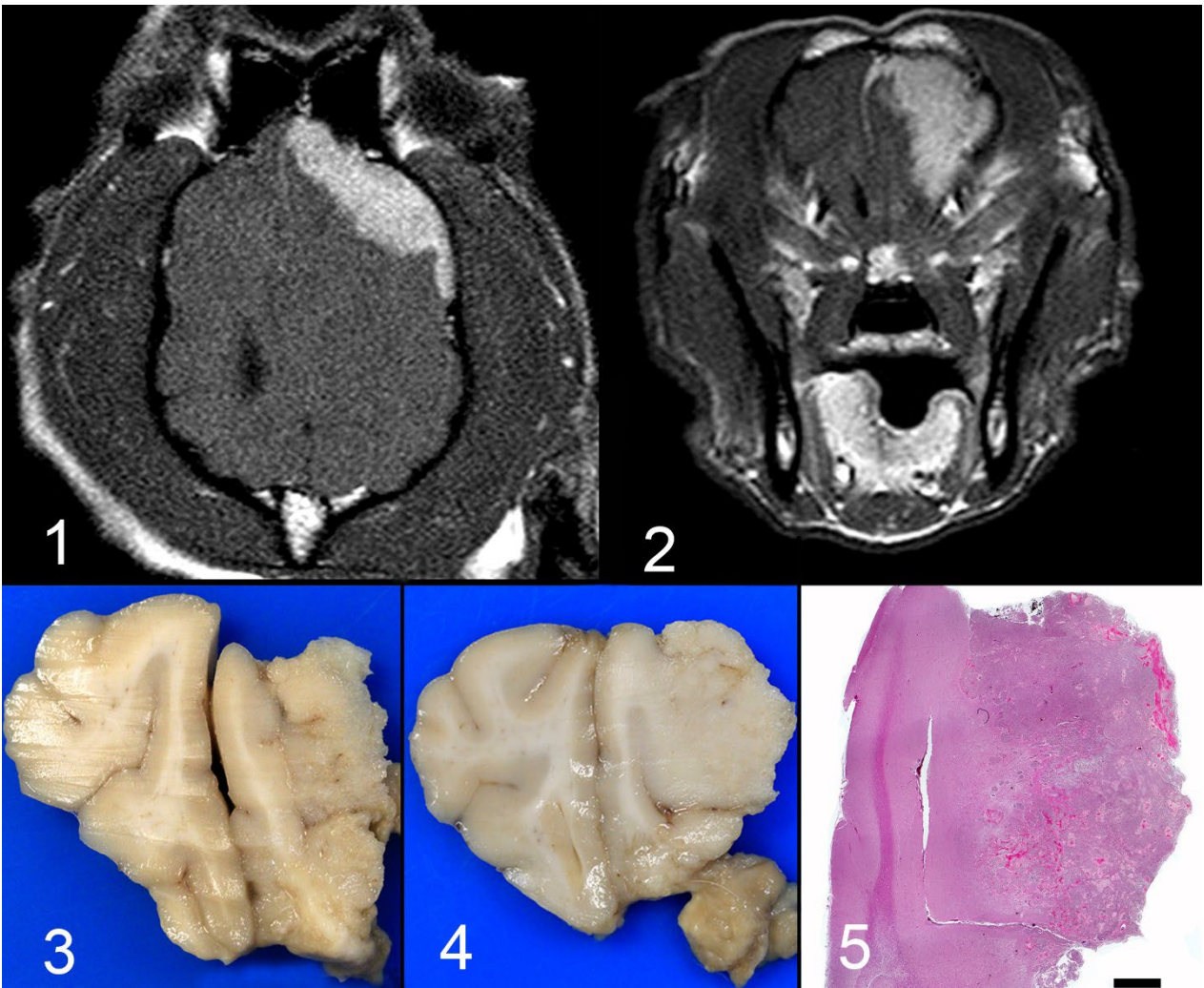


*Figure 1-1. Cerebrum, dog. A plaque-like mass centered on the rostral surface of the right frontal lobe extends caudally along the parietal lobe and medially along the falx cerebri (Fig 1,2). The right frontal lobe has a firm tan, mass that is adhered to the dura and measures 2.3 x 3 x 3.3 cm. The regional cerebral gyri are expanded (edema). (Fig 3-5).*

thickening of the meninges.<sup>2</sup> GCTs are typically unilateral, which can result in midline shifts caused by cerebral edema (as in this case). There are few reports of GCTs in the peripheral nervous system of dogs.<sup>4</sup> These tumors are characteristically comprised of large cells with abundant, granular eosinophilic cytoplasm.<sup>2</sup> The granular appearance of the cytoplasm is thought to be due to the presence of abundant lysosomes.<sup>2</sup> The cell of origin is unknown and is disputed in the literature.<sup>2,5</sup> It has been suggested that GCTs represent a common phenotype expressed by a variety of tumor cells.<sup>1,3</sup> Tumors that can exhibit granular changes are many and include meningiomas and other primary tumors of the CNS, paragangliomas, schwannomas, neurofibromas, leiomyomas, hibernomas, fibroxanthomas and rhabdomyomas.<sup>4</sup> In humans, peripheral GCTs are of Schwann cell origin, while intracranial GCTs are derived from astrocytes and pituicytes,<sup>5</sup> commonly occurring within the infundibulum or neurohypophysis.<sup>3</sup> Granular cells are frequently observed in other types of primary brain tumors,<sup>2</sup> which may reflect a nonspecific metabolic transformation.<sup>3</sup> A granular cell component has been reported in some human astrocytomas, meningiomas, and oligodendrogliomas.<sup>3,5</sup>

The imaging appearance of this tumor is characterized by strong, uniform, contrast enhancement and T1 weighted hyperintensity, as observed in this case.<sup>2</sup> The presence of T1 weighted hyperintensity in GCTs is considered a useful diagnostic feature.<sup>2</sup> These tumors can also be hyperintense on T2 weighted and FLAIR images,<sup>1,2</sup> however, this mass was predominantly T2 isointense to faintly hypointense with patchy FLAIR hyperintensities. Additional useful imaging features include a plaque-like distribution pattern, peritumoral edema with a mass effect, meningeal involvement and an absence of bone involvement.<sup>1</sup> These characteristics are not unique to the GCT, thus must be interpreted with caution, as GCT represents an extremely rare neoplasm of the canine central nervous system.<sup>1</sup>

Granular cell tumors typically stain strongly with PAS and are diastase resistant.<sup>1-5</sup> With immunohistochemistry, the granules are immunoreactive for ubiquitin,<sup>2,3</sup> with variable immunoreactivity for Vimentin, S-100,  $\alpha$  1-antichymotrypsin and  $\alpha$  1-antitrypsin.<sup>2,3</sup> GCTs are consistently negative for GFAP, pancytokeratins, leukocyte and macrophage markers.<sup>3</sup> The uniform positive ubiquitin staining may indicate cytosolic proteasome degradation activated by ubiquitin dependent

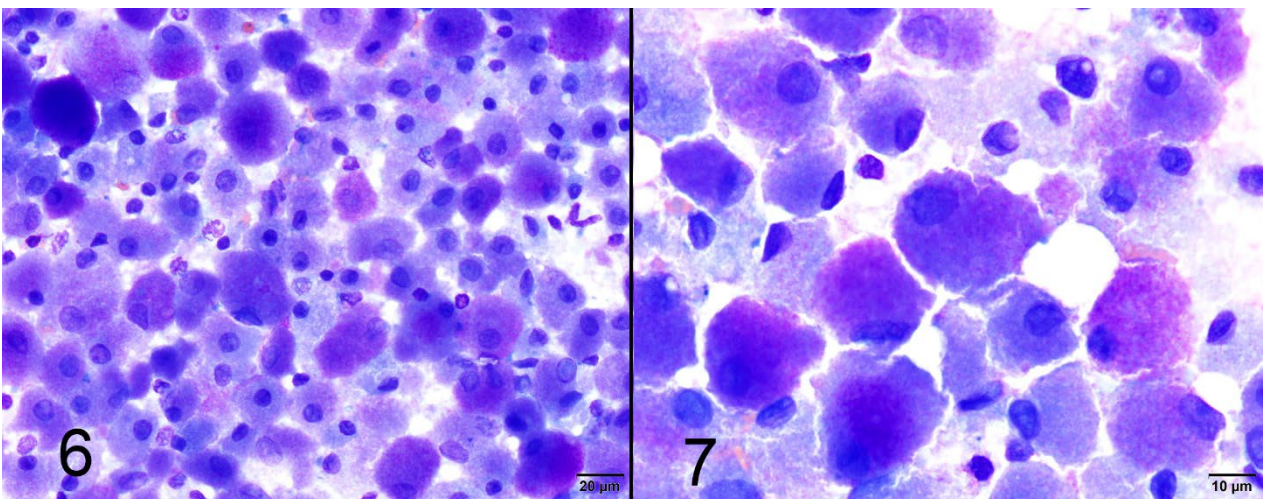
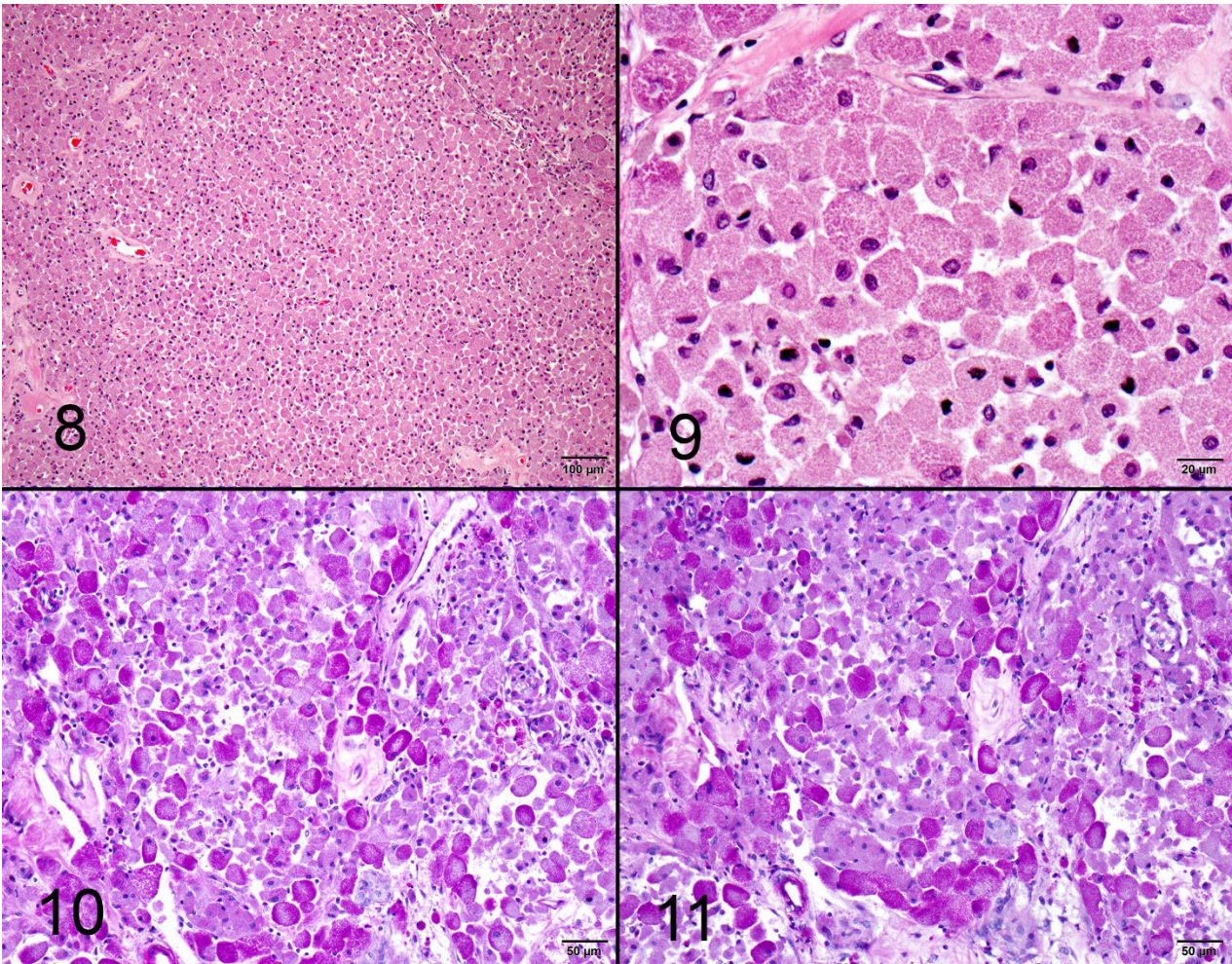


Figure 1-2. Cerebrum, dog. Impression smears of the mass. (Photo courtesy of: Animal Medical Center, 510 East 62<sup>nd</sup> St. New York, NY 10065. <http://www.amcnny.org>)

processes or breakdown of proteins facilitated by protein-ubiquitin conjugates mediated by the endosome-lysosome system.<sup>3</sup> Staining of granules with anti-proteinases ( $\alpha$ -1 antitrypsin and chymotrypsin) was initially thought to reflect a possible histiocyte origin, however, these findings are of limited specificity and histiocytic origin is not considered likely.<sup>3</sup> Ultrastructural evaluation reveals that the granular cytoplasm contains densely packed autophagosomes containing residual and dense bodies, irregular and membrane bound granules, multivesicular bodies, empty vesicles and membrane-like whorls.<sup>2,3</sup> Lysosomal accumulation is thought to be secondary to cellular degeneration, lysosomal enzyme defects and autophagy.<sup>5</sup> Schwann or

meningeal cell origin is considered less likely due to the lack of desmosomal or gap junctions as well as peripheral basal lamina.<sup>2</sup>

Fibrosis was prominent in the regional leptomeninges in this case, and the presence of abundant collagenous tissue has been previously reported in canine GCTs.<sup>3</sup> In one case series, spindle shaped cells entrapped within collagenous tissue were hypothesized to transition to the large granular cells outside of the collagenous extracellular matrix.<sup>3</sup> GCTs grow slowly and rarely metastasize,<sup>4</sup> and in this case, the tumor was documented to be present for a period of 2 years following radiation therapy. These tumors are described in numerous other species, including people,



**Figure 1-3. Cerebrum, dog. The neoplasm is comprised of large round, oval and polygonal cells in sheets. (Figs. 8,9) Cytoplasmic granules are PAS positive (Fig 10) and diastase resistant (Fig 11) (Photo courtesy of: Animal Medical Center, 510 East 62<sup>nd</sup> St. New York, NY 10065. <http://www.amcny.org>)**

horses, rats, cats, ferrets and birds.<sup>5</sup> Common locations include the lungs in horses, the tongue in dogs and the meninges in rats.<sup>5</sup> In rats, GCTs are the most common primary CNS tumor.<sup>1,3,4</sup> Ultrastructural and morphological evidence in rats suggests that intracranial GCTs originate from arachnoid cells of the meninges.<sup>1,3</sup>

#### **Contributing Institution:**

Animal Medical Center, 510 East 62<sup>nd</sup> St.  
New York, NY 10065.

<http://www.amcny.org>

#### **JPC Diagnosis:**

Leptomeninges and cerebrum: Granular cell tumor.

#### **JPC Comment:**

There are a few recent publications on this uncommon neoplasm in novel species. This week's moderator, MAJ Daniel Finnegan, described a meningeal granular cell tumor in a green tree python.<sup>2</sup> Reifinger et al. documented another case of granular cell tumor in the abdominal cavity of a snake.<sup>6</sup> These cases both had PAS positive and diastase resistant cytoplasmic granules, confirmed to be phagolysosomes on electron microscopy. These were the first two documented granular cell

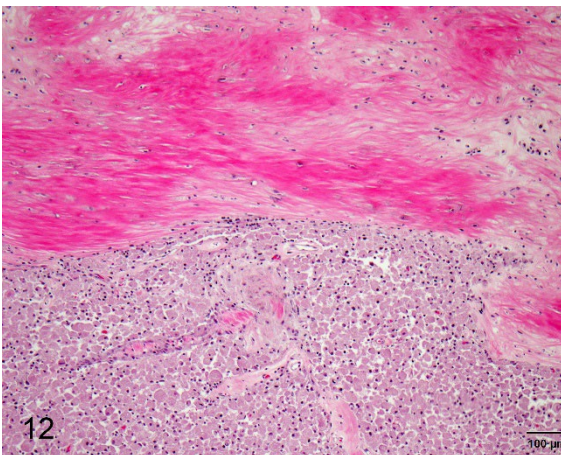


**Figure 1-4. Cerebrum, dog.** There is fibrosis of the leptomeninges which extends into the neoplasm (Fig. 12) (HE, 400X) (Photo courtesy of: Animal Medical Center, 510 East 62<sup>nd</sup> St. New York, NY 10065. <http://www.amcny.org>)

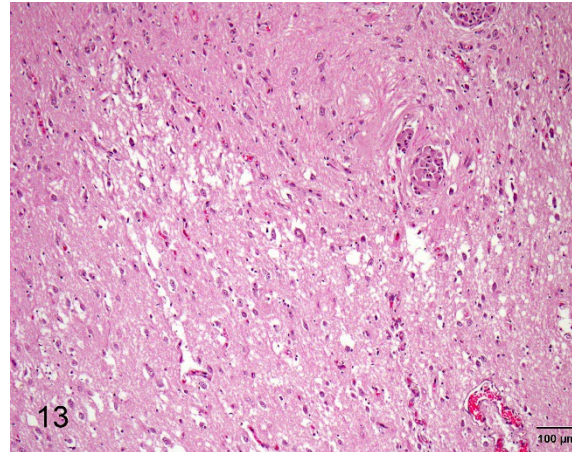


**Figure 1-5. Cerebrum, dog.** At the advancing edge of the neoplasm, there is parenchymal rarefaction and gliosis. (HE, 400X) (Photo courtesy of: Animal Medical Center, 510 East 62<sup>nd</sup> St. New York, NY 10065. <http://www.amcny.org>)

tumors in snakes, and granular cell tumors are rarely reported in non-mammalian species.

Granular cell tumors are characteristically compressive and non-infiltrative neoplasms. This case is unique in its infiltrative growth pattern; the moderator and participants discussed that this might be due to the chronicity or size of the neoplasm.

The contributor described the common presentations of granular cell tumors in mammalian species. A recent study demonstrated the propensity for rabbits to develop testicular granular cell tumors.<sup>7</sup> In 52 rabbits with testicular tumors, 63% were granular cell tumors, and 11 of 36 had bilateral granular cell tumors.<sup>7</sup> While other studies cite interstitial cell tumors as the most common testicular tumor in rabbits, this study suggests that granular cell tumors may be more common.

#### **References:**

1. Anwer, C.C., Vernau, K.M., Higgins, R.J., et al. Magnetic resonance imaging features of intracranial granular cell tumors in six dogs. *Vet Radiol Ultrasound* 2013; **54**:271–277.

2. Finnegan DK, Cartoceti AN, Hauck AM, LaDouceur EEB. Meningeal Granular Cell Tumor in a Green Tree Python (*Morelia viridis*). *J Comp Path.* 2020; 174: 54-57.
3. Higgins RJ, Bollen AW, Dickinson PJ, Siso-Llonch, S. Tumors of the Nervous System. In: *Tumors in Domestic Animals*, 5<sup>th</sup> Ed. Ames, IA: John Wiley & sons, Inc; 2017:870-872.
4. Higgins, R.J., LeCouteur, R.A., Vernau K.M., et al. Granular cell tumors of the canine central nervous system: two cases. *Vet Pathol* 2001; **38**:620–627.
5. Rao, D., Rylander, H., Drees, R., et al. Granular cell tumor in a lumbar spinal nerve of a dog. *J Vet Diagn Invest* 2010; **22**:638–642.
6. Reifinger M, Dinhopf N, Gumpengberger M, Konecny M, Cigler P. Granular Cell Tumour in a California Kingsnake. *J Comp Path.* 2020; 175: 24-28.
7. Reineking W, Seehusen F, Lehmbecker A, Wohlsein P. Predominance of Granular Cell Tumors among Testicular Tumours of Rabbits (*Oryctolagus cuniculi* f. dom.). *J Comp Path.* 2019; 153: 24-29.
8. Spoor MS, Kim DY, Kanazono S. et al. What is your diagnosis? Impression smears of a cerebral mass from a dog. *Vet Clin Pathol* 2013; **42**(2):240-241.

## **CASE II:**

### **Signalment:**

7-month-old, female spayed, boxer dog (*Canis familiaris*)

### **History:**

The patient presented to their veterinarian for a 3-month history of pollakiuria characterized by voiding small volumes of urine every 30-60 minutes. Cystocentesis of the patient's bladder yielded small quantities of foul-smelling urine which upon urinalysis, con-

tained markedly increased numbers of leukocytes (pyuria) and erythrocytes (hematuria). Aerobic bacterial culture of the urine isolated large numbers of *Escherichia coli*. Despite antibiotic therapy for several weeks, pollakiuria persisted. Ultrasonographic and radiographic assessment of the urinary bladder revealed a severely and irregularly thickened bladder mucosa; there was no overt evidence of cystoliths. An incisional biopsy of the urinary bladder was taken and submitted for histopathology.

### **Gross Pathology:**

The bladder mucosa was markedly thickened by multifocal-to-coalescing, poorly demarcated, firm, pale tan, polypoid masses.

### **Laboratory Results:**

No laboratory results reported.

### **Microscopic Description:**

Urinary bladder: Expanding the superficial aspect of the urinary bladder lamina propria and elevating the overlying urothelium is a large, poorly demarcated, densely cellular, plaque-like mass composed of dense sheets of large macrophages. These large macrophages have abundant cytoplasm that are packed with innumerable coarse eosinophilic granules and frequently contain one to three, 5-15 µm, pale eosinophilic, finely granular intracytoplasmic inclusions. Multifocally scattered throughout the dense sheets of macrophages are small aggregates of lymphocytes, plasma cells, and neutrophils. The

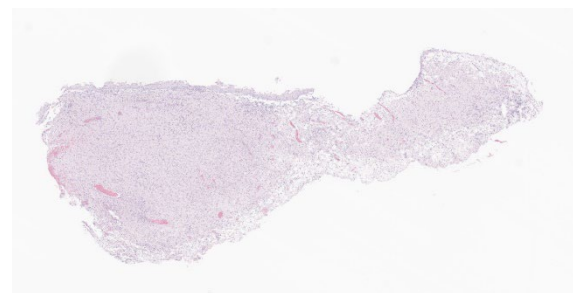


**Figure 2-1. Urinary bladder, dog. A section of urinary bladder contains a mildly hyperplastic mucosa overlying a markedly expanded submucosa. (HE 6X)**

urothelium overlying the mass is multifocally eroded and has small-to-moderate numbers of lymphocytes and neutrophils percolating throughout. The lamina propria underlying the mass is moderately expanded by clear to pale eosinophilic wispy fluid (edema).

100% of the large macrophages comprising the plaque-like mass exhibit strong cytoplasmic and membranous immunolabelling with Iba1.

The intracytoplasmic granules and inclusions within the macrophages are all strongly PAS-positive. The granules and inclusions do not stain positively with Toluidine blue, Luxol fast blue, Giemsa, Von Kossa, or Prussian blue stains. There is no overt evidence of acid-fast organisms within these macrophages upon application of Ziehl-Neelsen and Fite-Faraco stains.

#### **Contributor's Morphologic Diagnoses:**

Urinary bladder: Severe, locally extensive, chronic, granulomatous cystitis with myriad intracytoplasmic PAS-positive granules and

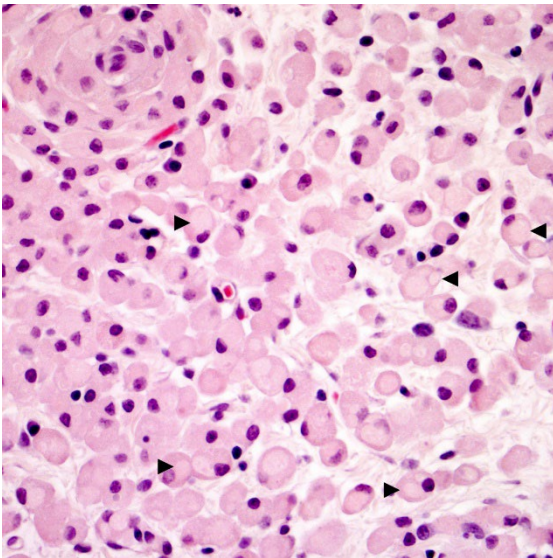


**Figure 2-2. Urinary bladder, dog. The submucosal infiltrate is composed of numerous macrophages (HE, 400X).** (Photo courtesy of: Cornell University School of Veterinary Medicine; <https://www.vet.cornell.edu/departments/biomedical-sciences/section-anatomic-pathology>).

inclusions, lamina propria edema, and multifocal epithelial erosion

#### **Contributor's Comment:**

Histopathology of the submitted urinary bladder mass revealed expansion of the lamina propria by a large plaque-like aggregate of large macrophages filled with abundant intracytoplasmic PAS-positive granules and inclusions. These microscopic findings, when viewed in conjunction with the signalment of the patient and the submitted clinical history, were deemed most consistent with a diagnosis of malakoplakia. Granular cell tumor and mycobacteriosis were also considered differential diagnoses prior to positive immunohistochemistry results for Iba1 (discounting a granular cell tumor) and the absence of overt acid-fast organism upon application of additional histochemical stains (discounting mycobacteriosis).

Malakoplakia is an uncommon granulomatous disease that has been reported in several veterinary species including dogs<sup>2,3,6,123</sup> cats<sup>1,4,10</sup>, pigs<sup>7,14</sup>, and a *Cynomolgus* macaque (*Macaca fascicularis*)<sup>11</sup>. Malakoplakia typically manifests within the genitourinary tract (particularly the urinary bladder) but has been reported in a variety of other body systems<sup>7,14,15</sup>. In humans, most cases of malakoplakia occur in middle-aged women, with infrequent cases reported in children<sup>15</sup>. In the seven previously reported cases of malakoplakia in dogs, all seven cases occurred in females with ages ranging from 6-weeks-old to 8-months-old<sup>2,3,6,13</sup>. In all of the other spontaneously occurring veterinary cases in which the full signalment was reported, all animals were female<sup>4,9,14</sup>.

While the exact etiopathogenesis of malakoplakia is still unclear, it has been putatively associated with recurrent bacterial infections, with the most commonly isolated bacteria be-

ing *E. coli* (as in the present case)<sup>15</sup>. It is postulated that females are over-represented in the current literature as they are more susceptible to urinary tract infections than males<sup>5</sup>. Immunosuppression has also been implicated as a contributing factor in the development of this disease as many human patients with malakoplakia are ailed by concurrent conditions that debilitate the immune system (e.g. acquired immunodeficiency syndrome and neoplasia) or are receiving immunosuppressive therapy<sup>15</sup>.

Grossly, malakoplakia appears as firm tan to yellow-brown masses that vary in morphology from focal plaques to multifocal-to-coalescing nodules to locally extensive thickenings of the affected organ(s). The typical histological appearance of malakoplakia is exuberant granulomatous inflammation characterized by dense sheets of large macrophages filled with abundant intracytoplasmic PAS-positive granules and inclusions (so-called ‘von Hansemann-type macrophages’)<sup>15</sup>. Many have postulated that the PAS-positive

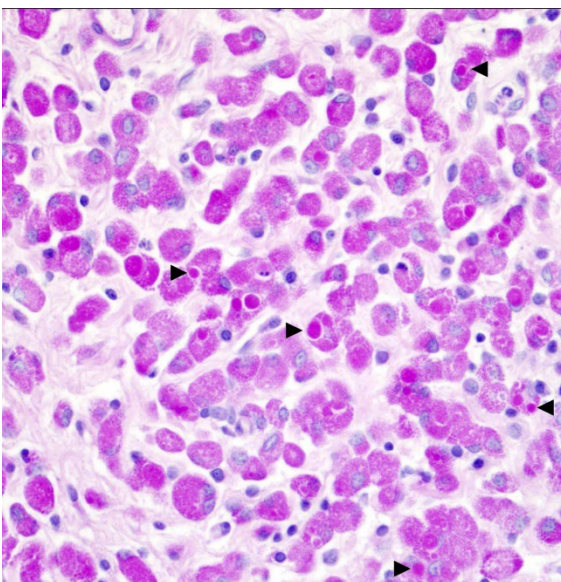


**Figure 2-3. Urinary bladder, dog. Macrophages contain numerous PAS-positive granules and inclusions (arrows). (PAS, 400X). (Photo courtesy of: Cornell University School of Veterinary Medicine; <https://www.vet.cornell.edu/departments/biomedical-sciences/section-anatomic-pathology>).**

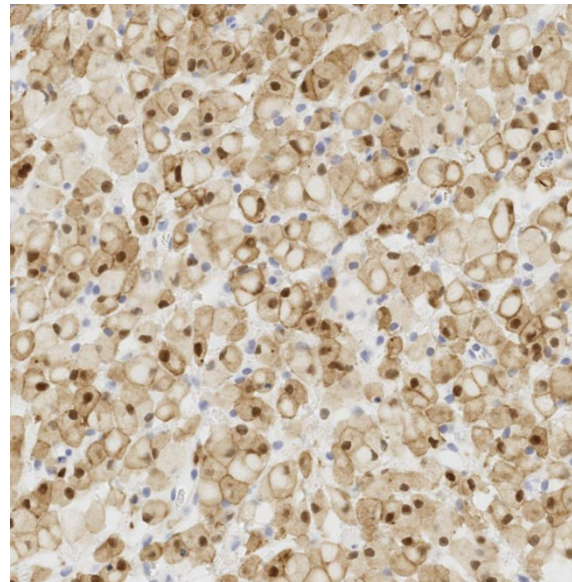


**Figure 2-4. Urinary bladder, dog. Macrophages demonstrate strong immunopositivity for IBA-1. (anti-IBA-1, 400X). (Photo courtesy of: Cornell University School of Veterinary Medicine; <https://www.vet.cornell.edu/departments/biomedical-sciences/section-anatomic-pathology>).**

granules and inclusions within these macrophages are the result of defective macrophage phagolysosome function and subsequent accumulation of bacterial breakdown products within the cytoplasm<sup>15</sup>. While not present in all cases, small numbers of 3-8  $\mu\text{m}$  basophilic intracellular and/or extracellular targetoid concretions termed ‘Michaelis-Gutmann bodies’ are scattered throughout regions of granulomatous inflammation; these concretions are thought to be pathognomonic for malakoplakia<sup>9</sup>. ‘Michaelis-Gutmann bodies’ stain positively with both Von Kossa and Prussian blue stains and are postulated to represent concretions of organic matter, iron, and calcium derived from bacterial breakdown products<sup>9</sup>. Von Kossa and Prussian blue stains did not highlight the presence of ‘Michaelis-Gutmann bodies’ in the present case.

The histological appearance of the macrophages within malakoplakia lesions are strikingly similar to those found in cases of granulomatous colitis of boxer dogs (GCB; also

known as histiocytic ulcerative colitis. GCB, similar to malakoplakia, is also associated with an exuberant granulomatous inflammatory response to *E. coli*<sup>11</sup>. It is salient to note that all seven reported cases of malakoplakia in dogs (including the present case) occurred in brachycephalic breeds that have been known to develop GCB (Boxer, Pug, English Bulldogs, Staffordshire Bull Terrier, and French Bulldog)<sup>2,3,6,13</sup>. The similarities between GCB and malakoplakia are intriguing and certainly strengthen the hypothesis that malakoplakia may arise in individuals that possess macrophages that are unable to eliminate certain *E. coli* pathotypes, resulting in persistent infections and macrophages becoming laden with PAS-positive bacterial products.

In summary, malakoplakia is an uncommon granulomatous disease that typically affects the genitourinary tract. Females, brachycephalic dog breeds, and young animals are over-represented in cases of malakoplakia within the current veterinary literature. While the exact etiopathogenesis of malakoplakia is unclear, both bacterial infection (namely *E. coli*) and immunosuppression are putatively associated with the development of this disease. Given the various similarities between malakoplakia and granulomatous colitis of

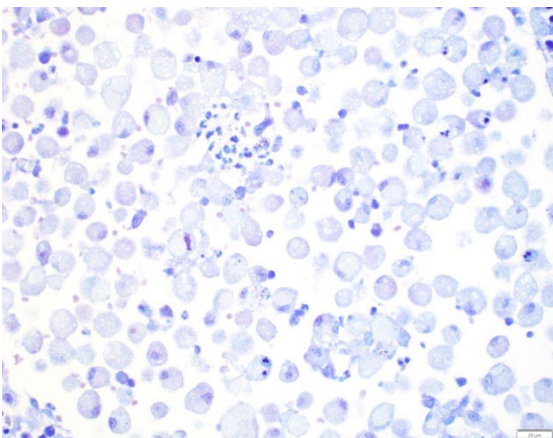


**Figure 2-5.** Urinary bladder, dog. Rare histiocytes contain aggregates of bacilli in their cytoplasm. (Giemsa, 300X)

boxer dogs (GCB), a genetic deficit that renders macrophages unable to eliminate certain *E. coli* pathotypes may also be involved in the development of malakoplakia. Malakoplakia should be considered a differential diagnosis for urinary bladder masses, especially in young female dogs with a history of bacterial cystitis.

#### **Contributing Institution:**

Department of Biomedical Sciences, Section of Anatomic Pathology  
College of Veterinary Medicine  
Cornell University  
Ithaca, NY  
USA

<https://www.vet.cornell.edu/departments/biomedical-sciences/section-anatomic-pathology>

#### **JPC Diagnosis:**

Urinary bladder, lamina propria: Cystitis, granulomatous, diffuse, severe.

#### **JPC Comment:**

The contributor provides an excellent comment on this uncommon condition in humans and select animal species. The term malakoplakia is derived from the Greek words for soft (*malacos*) and plaques (*placos*). The condition was first described by Michaelis, Gutmann, and von Hansemann in 1902-1903, and the key histologic features of this condition still bear their names.<sup>8</sup> Malakoplakia occurs more commonly in humans than in animals, though it is still rare. In humans, the condition has been documented in the urinary tract, gastrointestinal tract, gall bladder, pancreas, skin, reproductive tract (prostate, testes, cervix, vulva), lungs, and other tissues.<sup>15</sup> In the gastrointestinal system, the most commonly affected sites are the colon and rectum, and its occurrence in the colon has been associated with colon cancer.<sup>15</sup> Cutaneous malakoplakia more commonly occurs in adult

males and in organ transplant recipients on an immunosuppressive regimen.<sup>8</sup> Cutaneous lesions may present as papules, nodules, ulcers, or abscesses with draining tracts; occasionally, cutaneous lesions are associated with nonhealing surgical wounds.<sup>8</sup> While *E. coli* is the most commonly isolated organism in humans, certain types of patients may be prone to developing malakoplakia with a different organism. *Rhodococcus equi*, for instance, is commonly found in patients with acquired immunodeficiency syndrome.<sup>15</sup>

### References:

1. Bayley C, Slocombe R, Tatarczuch L. Malakoplakia in the urinary bladder of a kitten. *J Comp Pathol.* 2008;139(1):47-50.
2. Benzimra C, Job C, Pascal Q, Bureau S, Combes A, Bongrand Y, R. Faucher M. Malakoplakia of the bladder in a 4-month-old puppy. *J Am Anim Hosp Assoc.* 2019;55(5):261-5.
3. Brückner M. Malakoplakia of the urinary bladder in a young French Bulldog. *J Am Vet Med Assoc.* 2022;260(5):543-8.
4. Cattin RP, Hardcastle MR, Simpson KW. Successful treatment of vaginal malakoplakia in a young cat. *J Feline Med Surg Open Rep.* 2016;2(2). doi:10.1177/2055116916674871
5. Cianciolo RE, Mohr FC. Urinary system. In: Maxie GM, ed. *Jubb, Kennedy, & Palmer's Pathology of Domestic Animals.* 6th ed. Elsevier; 2015:459–461.
6. Davis KL, Cheng L, Ramos-Vara J, Sánchez MD, Wilkes RP, Sola MF. Malakoplakia in the urinary bladder of 4 puppies. *Vet Pathol.* 2021;58(4):699-704.
7. Gelmetti D, Gibelli L, Gelmini L, Sironi G. Malakoplakia with digestive tract involvement in a pig. *Vet Pathol.* 2014;51(4):809-11.
8. Kohl SK, Hans CP. Cutaneous Malakoplakia. *Arch Pathol Lab Med.* 2008; 132: 113-117.
9. Lewin KJ, Fair WR, Steigbigel RT, Winberg CD, Droller MJ. Clinical and laboratory studies into the pathogenesis of malakoplakia. *J Clin Pathol.* 1976;29(4):354-63.
10. Rutland BE, Nimmo J, Goldsworthy M, Simcock JO, Simpson KW, Kuntz CA. Successful treatment of malakoplakia of the bladder in a kitten. *J Feline Med Surg.* 2013;15(8):744-8.
11. Simpson KW, Dogan B, Rishniw M, Goldstein RE, Klaessig S, McDonough PL, German AJ, Yates RM, Russell DG, Johnson SE, Berg DE. Adherent and invasive *Escherichia coli* is associated with granulomatous colitis in boxer dogs. *Infect Immun.* 2006;74(8):4778-92.
12. Taketa Y, Inomata A, Sonoda J, Hayakawa K, Nakano-Ito K, Ohta E, Seki Y, Goto A, Hosokawa S. Granulomatous nephritis consistent with malakoplakia in a cynomolgus monkey. *J Toxicol Pathol.* 2013;26(4):419-22.
13. Tang KM, Serpa PB, Santos AP. What is your diagnosis? Urine from a dog. *Vet Clin Pathol.* 2022. doi:10.1111/vcp.13139.
14. Taniyama H, Ono T, Matsui T. Systemic malakoplakia in a breeding pig. *J Comp Pathol.* 1985;95(1):79-85. (9)
15. Yousef GM, Naghibi B. Malakoplakia outside the urinary tract. *Arch Pathol Lab Med.* 2007;131(2):297-300. (11)

### CASE III:

#### **Signalment:**

9-year-old spayed female canine (*Canis familiaris*)

#### **History:**

Patient presented 6 months before for a mass in the ventral neck. It was diagnosed as a possible abscess and Clavamox and Baytril were prescribed.

Today, patient presented for recheck with no improvement noted. She has difficulty walking, generalized weakness and is hesitant to move. She is painful (4/5) and anxious (4/5). Differential diagnosis includes IVDD.

### **Gross Pathology:**

The submandibular lymph nodes are enlarged bilaterally and asymmetrically. The left lymph node (7 x 3 x 2 cm) starts at the mandibular ramus, is firm, movable and dark red in color. The right lymph node (4 x 1.5 x 1 cm) has the same appearance. The cranial mediastinal lymph nodes are dark red in color, firm and enlarged (3 x 1, 5 x 4 cm nodules). On cut section, all the affected lymph nodes are solid, firm, and diffusely red. The lymph node architecture is partially effaced. Severe degree of spondylosis T13-L1, L2-L3, L4-L5 and L-S junction, extending into the vertebral canal. The ventral thoracic vertebrae also show a mild degree of spondylosis. No IVDD was found.

### **Laboratory Results:**

No laboratory results reported.

### **Microscopic Description:**

Lymph node, one section. Approximately 90% of the entire architecture is effaced by an expansile area characterized by locally extensive proliferation of anastomosing, variable sized and dilated slit openings resembling vascular channels. These channels are lined by plump endothelial cells. There are small



*Figure 3-1. Mandibular lymph node, dog. A single transverse section of lymph node is submitted for examination. Approximately 50% of the node is effaced and markedly congested. (HE, 6X)*

areas of necrosis, characterized by intense eosinophilic, amorphous material, admixed with scattered macrophages, rare lymphocytes and plasma cells. These vascular channels are filled with RBCs and scattered clusters of neutrophils and macrophages. Pigment-laden macrophages are common throughout (hemosiderin). The remaining normal nodal architecture is compressed with cortex and paracortex characterized by coalescing lymphoid follicles with starry sky appearance (tingible body macrophages). The lymphoid follicles have prominent germinal centers.

### **Contributor's Morphologic Diagnoses:**

DDX: Lymph node: locally extensive vascular proliferation with lymphoid atrophy compatible with nodal plexiform vasculopathy.

### **Contributor's Comment:**

Benign, non-neoplastic and neoplastic vascular proliferations in the lymph nodes have been described in different animal species.

The differential diagnosis for vascular proliferations in a lymph node includes nodal angiomatosis, plexiform vasculopathy, nodal hemangioma, nodal vascular hamartoma, and nodal telangiectasis. All of them are of unknown cause and usually present as incidental, benign proliferations that will efface and replace the normal lymphoid architecture.

Plexiform vasculopathy, also known as vascular transformation of lymph nodes, is an endothelial proliferation within lymph nodes and has been reported in humans, cats, and one dog with thyroidal carcinoma.<sup>5</sup> It is an uncommon lesion, and it is still unknown whether the proliferating endothelial cells are of lymphatic or blood origin. The literature describes it as a lymphadenopathy with vasoproliferation and lymphoid atrophy.<sup>7</sup> The lesions are usually focal but can involve most

of the lymphoid tissue. The lesions are distinct from more common findings such as lymphosarcoma, reactive lymphadenopathies, and normal lymph nodes.

The pathogenesis of this disease is unclear in both the human and animal literature.

The description of plexiform vasculopathy has been limited to cats. The human equivalent to this disease is nodal angiomatosis. There is one paper that describes a lymphadenopathy in a dog associated with thyroid carcinoma. The histological description was similar to that of nodal angiomatosis and plexiform vasculopathy.<sup>3</sup>

Clinical signs are nonspecific and generally present as secondary signs to some sort of lymphadenopathy in the cervical or inguinal region. Lymph nodes are enlarged and in cross section they have a fleshy tan to purple appearance.<sup>7</sup> Some of these signs include dyspnea, nonpainful masses, and difficulty swallowing. Histopathology shows severe loss of lymphoid tissue distributed throughout the lymph node and replaced by accumulations of erythrocytes within a capillary-like

proliferation of endothelial cells. The endothelial cells are characterized by small, elongated, basophilic nuclei and inconspicuous cytoplasm. Mitotic figures were rare throughout.<sup>5,7</sup>

Cytoplasmic expression of CD31 and factor VIII-related antigens were found via immunohistochemistry in all proliferated intranodal endothelial cells. A recent study used the lymphendothelial-specific marker, Prox-1, to determine the origin of the intranodal endothelial cells. The results of this study determined that the proliferative endothelial cells were of lymphatic origin.<sup>5</sup>

There are a variety of possible pathogenic explanations for plexiform vasculopathy including disturbances in drainage caused by tumors in the lymph node, thrombosis, severe congestive heart failure, or angiogenic factors released by a neoplastic process. A similar lesion of lymphatic proliferation has been experimentally induced in rabbits via incomplete occlusion of veins combined with complete obstruction of lymphatics, or just by the complete obstruction of lymphatics.<sup>5</sup> The

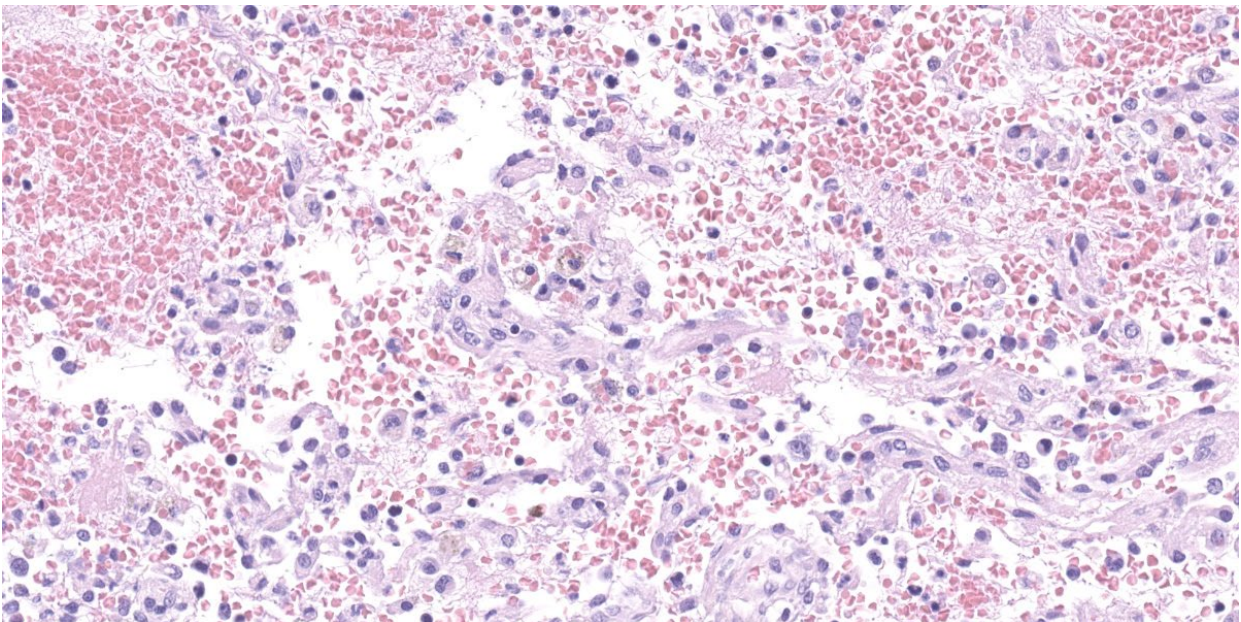


**Figure 3-2. Mandibular lymph node, dog. Proliferations of endothelial cells form blood filled vascular channels within affected areas of the node. (HE, 372X)**

later stages of human Acquired Immune Deficiency Syndrome (AIDS) is characterized by progressive lymphoid atrophy with vascular proliferation. However, the vascular proliferation associated with AIDS involves post-capillary venules with subsequent severe immune deficiency which does not occur in plexiform vasculopathy.<sup>7</sup>

Differentials should include other intranodal vascular proliferations such as angiomatous hamartoma, nodal lymphangiomas, hemolymph nodes, and nodal hemangiomas. However, none of these have been described in dogs.

Welsh et al. (1999) reported that complete excision of a retropharyngeal lymph node appears curative. Post-operative complications appeared to be limited to edema in the region of the excised lymph node.

**Contributing Institution:**

College of Veterinary Medicine, Western University of Health Sciences, 309 E. Second street  
Pomona, California 91766

<http://www.westernu.edu/xp/edu/veterinary/staff.xml>

**JPC Diagnosis:**

Lymph node: Vasculopathy and hemorrhage, severe, with marked fibrin deposition and extramedullary hematopoiesis.

**JPC Comment:**

Two major categories of non-neoplastic vascular proliferations within lymph nodes are angiomatous hamartoma and vascular transformation of sinuses.<sup>8</sup> In vascular transformation of sinuses, there is capillary proliferation within subcapsular and intermediate sinuses accompanied by variable amounts of fibrosis and lymphoid atrophy.<sup>8</sup> Variants of vascular transformation of sinuses include

plexiform vasculopathy, nodal angiomatosis in humans, and angiomatous hyperplasia in Wistar rats.<sup>8</sup> While not completely known, vascular transformation of sinuses is thought to occur due to occlusion of lymphatic or efferent veins which causes edema in the draining region. Plexiform vasculopathy is most commonly documented in the cervical lymph nodes of cats,<sup>5,9</sup> and in some cases, has been associated with malignant transformation to angiosarcoma.<sup>9</sup>

Angiomyomatous hamartoma, which has been documented in humans, a cynomolgus macaque, and a dog, involves proliferation of vessels with muscular walls within the cortex of the lymph node. The pathogenesis of angiomyomatous hamartoma is unknown. A recent report described the incidence of both angiomyomatous hamartoma within the hilus and vascular transformation within the subcapsular and medullary sinuses in the cranial mediastinal lymph nodes of a 1-year-old beagle in a toxicity study.<sup>8</sup>

This case generated significant discussion among the moderator and conference participants. In some regions of the node, the presence of well-defined plexiform channels is consistent with nodular plexiform vasculopathy. In other regions, collagen and smooth muscle actin within vascular walls (confirmed via histochemical and immunohistochemical staining) are more prominent than would be expected in plexiform vasculopathy

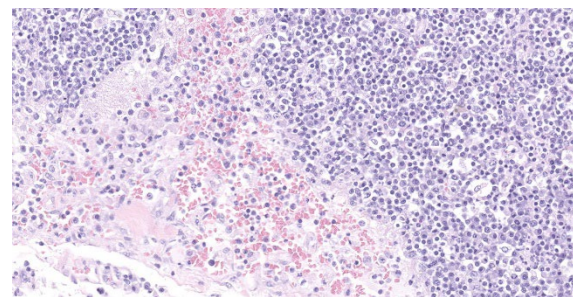


*Figure 3-3. Mandibular lymph node, dog. Vascular proliferation expands the subcapsular sinus. The adjacent cortex is moderately hyperplastic with numerous tingible body macrophages. (HE, 311X)*

but not enough to be consistent with a diagnosis of angio-myomatous hamartoma. The moderator and conference participants also discussed another prominent feature of this case: hemorrhage and fibrin thrombi. Participants discussed how polymerized fibrin can induce endothelial proliferation and fibrosis, and in this case, might serve as a potential cause for secondary vasculopathy within the node. Thus, hypercoagulability (i.e. due to protein losing nephropathy) was discussed as a potential differential.

Another differential considered less likely by the moderator and participants is neoplastic transformation. Hemangiomas are generally well circumscribed and expansile,<sup>8</sup> features which are lacking in this case. Hemangioendothelioma and hemangiosarcoma also feature a high mitotic rate, cellular atypia, and invasion.<sup>8</sup> Additionally, primary vascular neoplasia within lymph nodes is uncommon; in a study of 439 vascular tumors in dogs, only one primary tumor occurred in a lymph node, and only 2 of 63 angiosarcomas metastasized to lymph nodes.<sup>2</sup> In a separate study of 175 beagles that were controls in a toxicology study, however, hemangiomas were found incidentally in 9 popliteal and 1 hepatic lymph node, demonstrating that these may not be as uncommon as the literature suggests.<sup>4</sup>

Another feature discussed by the moderator and participants in this case is extramedullary hematopoiesis, consisting of lymphoid and erythroid precursors, megakaryocytes, and nurse cells.

#### References:

1. Fuji RN, Patton KM, Steinbach TJ, Schulman FY, Bradley GA, Brown TT, Wilson EA, Summers BA. Feline systemic reactive angioendotheliomatosis: eight cases and literature review. *Vet Pathol.* 42: 608-17.
2. Gamlem H, Nordstoga K, Arnesen K. Canine vascular neoplasia – a population based clinicopathologic study of 439 tumors and tumour-like lesions in 420 dogs. *APMIS.* 2018; Suppl 125: 41-54.
3. Gelberg HB, Valentine BA. Diagnostic exercise: Lymphadenopathy associated with thyroid carcinoma in a dog. *Vet Pathol.* 2011; 48(2), 530-534.
4. HogenEsch H, Hahn FF. Primary vascular neoplasms of lymph nodes in the dog. *Vet Pathol.* 1998; 35(1): 74-76.
5. Jungwirth N, Junginger J, Andrijczuk C, Baumgärtner W, Wohlsein P. Plexiform vasculopathy in feline cervical lymph nodes. *Vet Pathol.* 2018; 55 (3), 453-456.
6. Karim MS, Ensslin CJ, Dowd ML, Samie FH. Angiomyomatous hamartoma in a postauricular lymph node: A rare entity masquerading as a cyst. *JAAD Case Reports.* 2021; 7:131.
7. Lucke V, Davies JD, Wood CM, Whitbread TJ. Plexiform vascularization of lymph nodes: an unusual but distinctive lymphadenopathy in cats. *J Comp Pathol.* 1987; 97: 109-119.
8. Nelissen S, Chamanza R. An Angiomyomatous Hamartoma With Features of Vascular Transformation of Sinuses in the Mediastinal Lymph Node of a Beagle Dog. *Toxicol Pathol.* 2020; 48(8), 1017-1024.
9. Roof-Wages E, Spangler T, Spangler WL, Siedlecki CT. Histology and clinical outcome of benign and malignant vascular lesions primary to feline cervical lymph nodes. *Vet Pathol.* 2015; 52(2), 331-337.
10. Welsh EM, Griffon D, Whitbread TJ. Plexiform vascularization of a retropharyngeal lymph node in a cat. *J Small Anim Pract.* 1999; 40(6):291.

## **CASE IV:**

### **Signalment:**

An 8-month-old spayed female Boxer dog (*Canis familiaris*)

### **History:**

The dog was referred by a practitioner to a specialist veterinary center for management of acute spontaneous pneumothorax. On presentation to the specialist clinic the dog was tachypneic (64 bpm), hypoxemic (pulse oximetry 66% without oxygen supplementation, 92% with oxygen supplementation), and had increased respiratory effort with an abdominal component to the respiration. Lung sounds on the right side were dull on auscultation. Initial bloodwork revealed a mixed acidosis (pH 7.299; normal 7.35 – 7.45), with mild hemoconcentration (57%) and normal total solids (6.6 g/dl). Blood glucose was normal (4.7 g/dl), with no evidence of lactic acidosis (1.9 mmol/L; normal < 2.5 mmol/L).

Computed tomography (CT) showed multiple variably sized bullae in the right middle lung lobe, and partial or complete atelectasis of all remaining lung lobes. The dog was



**Figure 4-1. Right lung, dog.** There was bilateral pneumothorax at autopsy, with atelectasis of all lung lobes. (Photo courtesy of: Department of Veterinary Clinical and Diagnostic Sciences, Faculty of Veterinary Medicine, University of Calgary, 3280 Hospital Dr. NW, Calgary, Alberta T2N 4Z6, Canada, <http://vet.ucalgary.ca>)

anesthetized for surgery but died from cardiopulmonary arrest during pre-surgical thoracocentesis.

### **Gross Pathology:**

Necropsy examination revealed severe bilateral pneumothorax, with marked atelectasis of all lung lobes. The right middle lung lobe was small, pale and flaccid, with numerous collapsed, coalescing pleural bullae along its ventral and ventrocaudal margins; rupture of these bullae was presumed to be the source of the pneumothorax. The cartilage of the lobar bronchus supplying the right middle lung lobe was thin, flimsy and easily compressed when compared with bronchi supplying other lobes. In transverse section its lumen was slit-shaped rather than circular. In addition, an aberrant right subclavian artery arose in common with the left subclavian artery, forming a bisubclavian trunk. The right subclavian artery passed dorsal to the esophagus and compressed it.

### **Laboratory Results:**

No laboratory results reported.

### **Microscopic Description:**

This section from the right middle lung lobe is severely malformed and difficult to recognize as lung. It consists predominantly of a thick fibrovascular trabecular network outlining collapsed; empty spaces lined by a simple cuboidal to simple squamous epithelium. The lining epithelium is multifocally lost (autolytic artifact), and cystic spaces frequently contain rafts of sloughed epithelial cells. The fibrovascular trabeculae are variably thick, ranging in width from 20 to 300 microns, and contain many thin-walled blood vessels lined by mature endothelial cells, numerous mineralized areas, and scattered lymphoplasmacytic foci.

Multifocally, recognizable bronchiole-like structures are present. These are lined by simple cuboidal epithelium and have irregular bundles of smooth muscle in their walls. They are frequently adjacent to profiles of large arteries and veins (pulmonary vessels).

The section also contains a malformed bronchus surrounded by a nearly continuous layer of smooth muscle. Cartilage plates in this bronchus are irregular and present only around one half of the airway's circumference. The cartilage is immature, with small chondrocytes, less chondroid matrix and smaller lacunae (when compared with other lung sections from this dog and an age-matched control dog). Bronchial glands are fewer in number (when compared with other lung sections from this dog and the control dog).

**Contributor's Morphologic Diagnoses:**

Lung: Congenital pulmonary airway malformation (CPAM)-like lesion

**Contributor's Comment:**

The differential diagnosis for a single malformed lung lobe in a dog includes congenital



*Figure 4-2. Right lung, dog. The right middle lung lobe was small, pale and flaccid. (Photo courtesy of: Department of Veterinary Clinical and Diagnostic Sciences, Faculty of Veterinary Medicine, University of Calgary, 3280 Hospital Dr. NW, Calgary, Alberta T2N 4Z6, Canada, <http://vet.ucalgary.ca>)*



*Figure 4-3. Right subclavian artery, dog. The right subclavian artery passes dorsal to and compresses the esophagus. (Photo courtesy of: Department of Veterinary Clinical and Diagnostic Sciences, Faculty of Veterinary Medicine, University of Calgary, 3280 Hospital Dr. NW, Calgary, Alberta T2N 4Z6, Canada, <http://vet.ucalgary.ca>)*

lobar emphysema (CLE), a congenital pulmonary sequestration, and congenital pulmonary airway malformation (CPAM). Based on gross and histologic findings, the first two potential diagnoses can be ruled out in this dog. CLE requires overinflated alveoli or hyperplastic alveoli, whereas the affected lobe in this dog lacks alveoli. A congenital pulmonary sequestration lacks, by definition, any connection with the tracheobronchial tree. In this dog the affected lobe had a lobar bronchus, although it was flattened. Therefore, a presumptive diagnosis of CPAM-like lesion was made based on the similarity of this dog's lesions to described human lesions of CPAM and exclusion of other potential diagnoses.

The term CPAM refers to a spectrum of human airway malformations characterized by abnormal development of various portions of the tracheobronchial tree.<sup>16</sup> Formerly called congenital cystic adenomatoid malformations, CPAMs are well-recognized and relatively common in people. All types of CPAM are characterized by multiple irregular pulmonary cystic structures lined by varying types of epithelium. CPAMs in people are generally subdivided into five types based

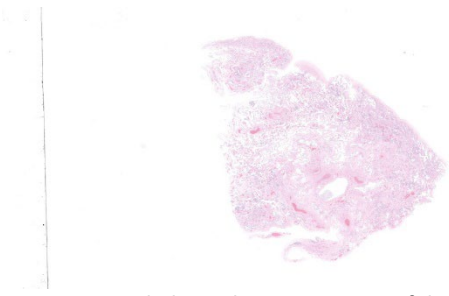


**Figure 4-4. Right lung, dog. One section of the right lung is submitted for examination. Normal alveolar architecture is not present. (HE, 7X)**

on the anatomic site of the malformation.<sup>16</sup> These are the: proximal tracheobronchial tree (type 0); bronchial/proximal bronchiolar region (type 1); bronchiolar region (type 2); terminal bronchiolar/alveolar duct region (type 3); and alveoli (type 4). There may be overlap between different types, and other classification systems have been proposed.<sup>11,13</sup>

The malformations in the dog in this case report shared overlapping features of human CPAM types 2 and 4. Type 2 CPAM is characterized by the presence of numerous 2-15 mm diameter parenchymal cysts. These consist of dilated bronchiole-like structures lined by cuboidal to columnar epithelium but with

mucus-producing cells generally absent. Other congenital abnormalities, including cardiovascular and renal malformations may be present in humans. (Interestingly, this dog had a malformation of the right subclavian artery, although the clinical significance of this was uncertain.) Type 4 CPAM is characterized by larger cysts, typically found toward the periphery of the lobe. These are lined by a mixture of flattened or rounded alveolar lining cells, and occasionally a low cuboidal epithelium. Both type 2 and type 4 human CPAMs typically affect a single lung lobe, as in this dog, and have a good prognosis after surgical resection.<sup>16,17</sup>

Like CPAM, congenital lobar emphysema (CLE) is also a well-recognized congenital lung malformation in humans.<sup>7,8,17</sup> It is characterized by overinflation of a single lung lobe due to partial obstruction of the bronchus supplying that lobe.<sup>10</sup> This obstruction can result from numerous causes, including malformation of the bronchus, external compression of the bronchus by masses or vascular anomalies, or internal obstruction of the

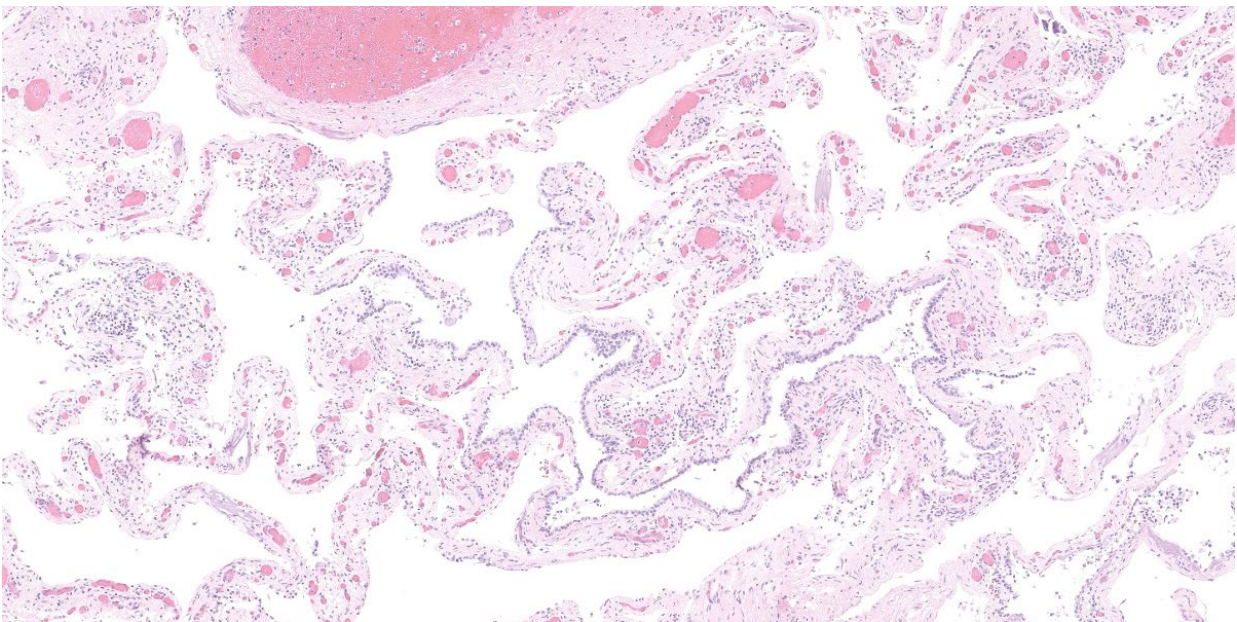


**Figure 4-5. Right lung, dog. The lobe is composed of airway-like structures lined by cuboidal epithelium separated by dense fibrous stroma. There is no alveolar parenchyma. (HE, 85X)**

bronchial lumen by mucus plugs or granulation tissue.<sup>8</sup> Regardless of the cause, the result is significant lobar overinflation as the partially obstructed bronchus acts as a one way valve and traps air. In the dog described in this case report the lobar bronchus was malformed and partially collapsed, consistent with one cause of CLE. However, in human CLE, alveoli are distended but are otherwise histologically normal, and fibrosis, inflammation or necrosis are rarely seen.<sup>8</sup> This is significantly different from the histologic lung changes in the dog described in this case report.

CLE has been previously reported several times in dogs,<sup>1,5,6,11,12,14,15,19,20</sup> and the dog described in this report has several features in common with many reported canine cases of CLE: the right middle lung lobe was affected; a bronchial structural abnormality was present; bullae and pneumothorax were a feature; and the dog was less than six months old. However, this dog's most significant histologic lesions (absence of recognizable alveolar architecture, with marked interstitial fibrosis) were incompatible with the simple alveolar hyperinflation expected in CLE. Seven human pediatric pathologists were consulted on this case and all agreed that this dog did have a congenital lung malformation and that it was not CLE.

This case highlights that there are multiple types of congenital lung malformations in dogs. It is possible that some reported canine cases of CLE may, in fact, represent CPAM-like lesions. Among published canine CLE reports, two describe histologic features that are suggestive of CPAM type 2<sup>4</sup> or type 4.<sup>11</sup> It may be that these were cases of CPAM-like lesions that were interpreted to be CLE, or that forms of pulmonary disease that share features of both diseases exist in dogs. There are numerous reports of human congenital lung lesions fulfilling criteria for both CPAM

and other congenital lung lesions,<sup>7</sup> and this may also prove to be the case in dogs.

It is important to recognize that not all congenital lung malformations in dogs are CLE, and that this diagnosis should not be made based solely on imaging or the gross appearance of an affected lung lobe; CPAM and CLE must be distinguished histologically. In humans there are practical clinical reasons for making an accurate diagnosis of congenital lung lesions. Most importantly, CPAM may progress to malignant neoplasia while CLE does not.<sup>5,7</sup> Lobectomy is generally indicated for CPAM lesions, while CLE may resolve spontaneously and can often be managed conservatively unless it causes mediastinal displacement or severe dyspnea.<sup>7</sup> Because CPAM-like disease in dogs has not been reported previously it is not possible to compare its treatment or prognosis with those of CLE.

#### **Contributing Institution:**

Department of Veterinary Clinical and Diagnostic Sciences

Faculty of Veterinary Medicine

University of Calgary

3280 Hospital Dr. NW

Calgary, Alberta T2N 4Z6

Canada

<http://vet.ucalgary.ca/>

#### **JPC Diagnosis:**

Lung: Congenital pulmonary airway malformation with mineralization.

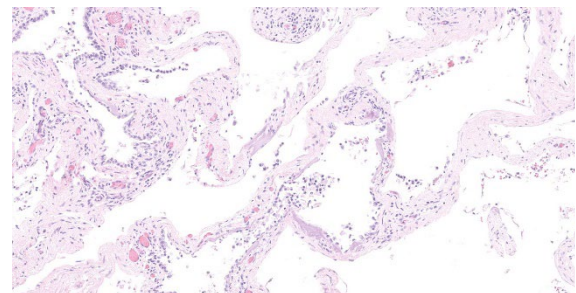


**Figure 4-6. Right lung, dog. There is multifocal mineralization of the stroma surrounding airway-like spaces. (HE, 7X)**

### JPC Comment:

The contributor provides an excellent review of congenital pulmonary airway malformations, congenital lobar emphysema, and the differences between the two diagnoses.

This week's moderator described the six stages of development of the lung: embryonic, pseudoglandular, canalicular, saccular, alveolar, and vascular maturation. Additionally, the moderator described that TTF-1 and HNF-3 are important transcription factors for early lung development.

Congenital pulmonary abnormalities in veterinary species are rare, and one of the more common conditions is accessory lung development in ruminants.<sup>2,9</sup> Accessory lungs are found in extrapulmonary locations, such as in the abdomen and subcutis.<sup>2,9</sup> These lobulated masses consist of haphazardly arranged and variably differentiated pulmonary elements, including bronchi lined by ciliated respiratory epithelium, alveoli, cartilage, and blood vessels.<sup>2,9</sup> While composed of similar elements, pulmonary hamartomas are different in that they are located within the lung. Pulmonary hamartomas are the most commonly diagnosed benign lung tumor in humans, typically discovered as incidental findings on radiographs, and are also occasionally seen in ruminants.<sup>2,3</sup> A recent article described a pulmonary hamartoma in a captive-bred, full-term elk calf found dead. The mass replaced the left caudal lung lobe, encompassed approximately half of the thorax, and compressed the remaining lungs.<sup>2</sup>

The moderator and conference participants also remarked on the presence of mineralization in this case; an explanation for mineralization was not readily apparent on H&E examination.

### References:

1. Billet JPHG, Sharpe A. Surgical treatment of congenital lobar emphysema in a puppy. *J Small Anim Pract.* 2002; 43: 84-87.
2. Boggiatto PM, Steven SC, Palmer MV. Pulmonary hamartoma in an elk calf. *J Vet Diagn Invest.* 2023; 3; 5(2): 193-195.
3. Caswell JL, Williams KJ. Respiratory System. In: Grant MG, ed. *Jubb, Kennedy, and Palmer's Pathology of Domestic Animals.* Vol 2. 6<sup>th</sup> ed. St. Louis, MO: Elsevier. 484-485.
4. Gopalakrishnan G, Stevenson GW. Congenital lobar emphysema and tension pneumothorax in a dog. *J Vet Diagn Invest.* 2007; 19: 322-325.
5. Hancock BJ, Dilorenzo M, Youssef S, Yazbeck S, Marcotte JE, Collin PP. Childhood Primary Pulmonary Neoplasms. *J Pediatr Surg.* 1993; 28: 1133-1136.
6. Herrtage ME, Clarke DD. Congenital lobar emphysema in 2 dogs. *J Small Anim Pract.* 1985; 26: 453-464.
7. Laberge J-M, Puligandla P, Flageole H. Asymptomatic congenital lung malformations. *Semin Pediatr Surg.* 2005; 14: 16-33.
8. Langston C. New concepts in the pathology of congenital lung malformations. *Semin Pediatr Surg.* 2003; 12: 17-37.
9. Lopez A, Martinson SA. Respiratory System, Thoracic Cavities, Mediastinum, and Pleura. In: Zachary JF, ed. *Pathologic Basis of Veterinary Disease.* 7<sup>th</sup> ed. St. Louis, MO: Elsevier. 2022; 570.
10. Mani H, Suarez E, Stocker JT. The morphologic spectrum of infantile lobar emphysema: a study of 33 cases. *Paediatr Respir Rev.* 2004; 5: S313-S320.
11. Matsumoto H, Kakehata T, Hyodo T, Hanada K, Tsuji Y, Hoshino S, Isomura H. Surgical correction of congenital lobar emphysema in a dog. *J Vet Med Sci.* 66: 217-219.

12. Moon H-S, Lee M-H, Han J-H, Kim S-K, Lee S-G, Lee L, Hyun C. Asymptomatic congenital lobar emphysema in a Pekinese dog. *Journal of Animal and Veterinary Advances*. 2007; 6: 556-558.
13. Puligandla PS, Laberge JM: Congenital Lung Lesions. *Clin Perinatol*. 2012; 39: 331-347.
14. Ruth J, Rademacher N, Ogden D, Rodriguez D, Gaschen L. Imaging diagnosis—congenital lobar emphysema in a dog. *Vet Radiol Ultrasound*. 2011; 52: 79-81.
15. Stephens JA, Parnell NK, Clarke K, Blevins WE, DeNicola D. Subcutaneous emphysema, pneumomediastinum, and pulmonary emphysema in a young schipperke. *J Am Anim Hosp Assoc*. 2002; 38: 121-124.
16. Stocker J. Congenital pulmonary airway malformation: a new name for and an expanded classification of congenital cystic adenomatoid malformation of the lung. *Histopathology*. 2002; 41: 424-431.
17. Stocker JT. Congenital and Developmental Diseases. In: Tomashefski Jr JF, ed. *Dail and Hammar's Pulmonary Pathology*. 3<sup>rd</sup> ed. New York: Springer Science. 2008.
18. Tennant BJ, Haywood S. Congenital bullous emphysema in a dog - a case report. *J Small Anim Pract*. 1987; 28: 109-116.
19. Voorhout G, Goedegebuure SA, Nap RC. Congenital lobar emphysema caused by aplasia of bronchial cartilage in a Pekingese puppy. *Vet Pathol*. 1986; 23: 83-84.
20. Yun S, Lee H, Lim J, Lee K, Jang K, Shiwa N, Boonsriro H, Kimitsuki K, Park C, Kwon Y. Congenital lobar emphysema concurrent with pneumothorax and pneumomediastinum in a dog. *J Vet Med Sci*. 2016; 78: 909-912.